Mini Review

Correlation Between Optical and Morphological Properties of Nanostructured Gold Thin Film

V. N. Rai* and A. K. Srivastava

Indus Synchrotrons Utilization Division, Raja Ramanna Centre for Advanced Technology, India

Abstract

This paper presents the study of optical properties and the morphology of the nanostructured gold thin films deposited on the glass substrate. The localized surface plasmon resonance (LSPR) peaks shift to higher wavelength side and reaches up to near infrared region with a controlled increase in the film thickness during its deposition. The shapes and sizes of the nanoparticles change with an increase in the film thickness. The roughness of the films increases, whereas the refractive index of the surrounding medium decreases with an increase in the film thickness. A correlation has been found between the LSPR wavelength, the surface morphology and the refractive index of the surrounding medium of the film. These thin films act as a substrate for surface enhanced spectroscopy and as a sensor for organic and biological samples.

INTRODUCTION

Plasmonics is an emerging branch of nano photonics that determines the properties of the collective excitation of free electrons in the thin films or in the nanoparticles of noble metal (Au and Ag) [1]. Generally, an interaction of electromagnetic waves with the thin films and/or nanoparticles (NPs) of Au and Ag excite localized surface plasmon resonance (LSPR), which provides strong extinction and scattering spectra that makes it useful for various important applications in different field of research [1-7] particularly in the field of biology and medicine. The LSPR frequency of NPs depends mainly upon the NPs size, shape, material properties and the surrounding medium [4, 5, 8-10]. The ability of NPs to integrate with biological samples has great impact in biology and medicine [11, 12]. Particularly, the gold NPs have attracted intensive interest because they are easily prepared, have low toxicity and can be readily attached to the molecules of biological and medicinal interest [13]. Therefore, it is important to control the optical properties of the composite medium (having metallic NPs and organic or biological samples) by careful selection of geometrical parameters of the NPs for various practical applications. Thus by selecting the distribution of sizes and shapes of the metallic NPs, it is possible to achieve enhanced absorption of the electromagnetic radiation in the specified spectral regions. The enhanced absorptions are the function of LSPR that produces high electromagnetic field near the nanoparticles, which forms the basis for surface enhanced

spectroscopy as a plasmonic sensor for the detection of organic and biological samples [3,14-20]. The gold nanoparticles (AuNPs) used for this purpose may be either in colloidal solution or in the form of nanostructured thin films.

The measurement of the LSPR absorption band in thin films allows the study of changes in the optical properties of the nanostructured materials. In fact any change in the optical properties of the thin film can be correlated with change in the dielectric properties (ε) of the materials, that is, the change in its refractive index (n) and the extinction coefficient (k) [4-5, 8], which are strongly dependent on the surface coverage of the films by the NPs. Recently, Chen and Horn [21] have studied the effective complex refractive index of a layer of AuNP adsorbed on to a silicon wafer at low surface coverage. They reported that the real and the imaginary components of the dielectric coefficient are the function of volume fraction of NPs in the layer. It has also been observed that the refractive index of the film increases linearly up to a volume fraction of 0.1. Wang et al., [22] have reported the dielectric trajectories of ultrathin gold film of thickness < 10 nm (from cluster to thin film) on silica. They found experimentally that the real part (n) of the film first increases and then decreases with an increase in the film thickness. It is an indication that the optical properties of the thin films are mainly dependent on the process of its preparation. Here it is important to mention that the hot cathode vacuum deposition process has been found as an easy and suitable technique for getting plasmonic thin films

---

Cite this article: Rai VN, Srivastava AK (2016) Correlation Between Optical and Morphological Properties of Nanostructured Gold Thin Film. JSM Nanotechnol Nanomed 4(1): 1039.

[23-25]. The nanostructures present in the films play a major role in deciding the optical properties of the films that are controlled largely by the process of its preparation. Even annealing of the thick films also produces different nanostructures in the films [24]. The effect of surface morphology of different types of films on its optical properties (LSPR) has been studied earlier and was found that the sizes of the NPs in x-y plane play an important role in deciding the optical properties of the thin films [25]. But still very less is known about the correlation between the LSPR and the surface structure of the thin films particularly its three dimensional sizes along with refractive index of the surrounding medium, which needs to be investigated systematically.

This paper provides a brief overview about the optical and structural properties of the nanostructured gold thin film to better understand the correlation between the surface structures (particularly the aspect ratio) of the NPs with the LSPR and the refractive index of the surrounding medium. Effect of surface roughness of the thin films on its optical properties is also discussed.

Experimental

The preparation of metallic nanostructured film for plasmonic application is critical because an enhancement in optical absorption (due to LSPR) is very much dependent on the size, shape and the particle density of NPs in the films. In fact, the deposition parameters of the film mainly affect the properties of these films such as the rate of film deposition, type of substrate, the substrate temperature and the required film thickness. For this experiment many gold films were deposited on the glass substrate (quartz glass slides) using vacuum evaporation technique. The vacuum deposition system was evacuated at chamber pressure of $\sim 3 \times 10^{-5}$ mbar using a diffusion pump. A resistively heated tungsten boat was used for evaporating the gold for thin film deposition. The thickness and the rate of deposition of the films were monitored by using a quartz crystal microbalance (QCM). For this purpose variation in the frequency of QCM was noted during the film deposition. The film thickness was estimated based on the shift in the frequency of QCM using standard formula having density of material deposited. The glass substrates were thoroughly cleaned before the film deposition in order to avoid the presence of any impurity on its surfaces. The substrate temperature, the deposition rate and the film thickness were the important parameters, which was controlled during the film deposition. These parameters decide the morphology of the films as well as its optical properties, particularly the LSPR frequency [19, 25]. The deposition parameters for the films were chosen as 25^0 C, < 0.01 Å s^{-1} and 5-150 Å respectively. The LSPR frequency is very much sensitive to the film deposition rate. This is the reason, the deposition rate was kept very slow (~ 0.01 Å s^{-1}) in order to grow individual/separated gold islands. The tungsten boat was slowly heated for each deposition such that the vaporized gold got deposited on the glass substrate before melting of the gold. The system was allowed to cool gradually near to room temperature after film deposition. It was found that the variation in the film thickness (measured using QCM) and its LSPR peak follow the theoretically obtained expression (scaling) reported earlier [25]. A good agreement between experimental values and the theoretical expression up to ~ 10 nm thickness

shows that once the substrate temperature and deposition rate were kept constant, the deposited films provided similar characteristics. However, the films having thickness more than 10 nm loses its NP character and becomes percolated films (semi-continuous/continuous) and does not provide a good LSPR peak.

The optical absorption spectra of the gold thin films were recorded in transmission mode using UV-Vis spectrophotometer (Lambda 20 Perkin Elmer) in order to find information about the LSPR. The spectra were recorded in the wavelength range from 400 – 1000 nm in the steps of ~ 0.3 nm with a resolution of ~ 0.1 nm. The shapes and sizes of the nanoislands were determined by transmission electron microscopy (TEM) and atomic force microscopy (AFM). The TEM measurements were carried out on the PHILIPS CM-200 microscope equipped with LaB$_6$ filament. The line resolution of the microscope was ~ 1.4 Å. Finally, surface morphology of the films was measured using an atomic force microscope (NT-MDT, SOLVER- PRO) having Si cantilever tips (resonant frequency-190 KHz, spring constant ~ 5.5 N/m) in non-contact mode, where radius of curvature of the tip was ~ 20 nm.

RESULTS AND DISCUSSION

Optical Properties of the gold thin films

The absorption spectra of gold nanostructured films of thickness ranging from ~ 0.5 - 15 nm were recorded in the wavelength range from 400 – 1000 nm (Figure 1) and the localized surface plasmon resonance (LSPR) wavelengths were assigned to the absorption maximum in each spectrum. Here the absorption spectrum of ~ 15 nm thick film is not shown in Figure (1). These spectra provided the LSPR peaks ranging from 536 – 962 nm and shifting towards higher wavelength side with an increasing bandwidth as the thicknesses of the films were increased from ~ 0.5 to 15 nm respectively (Figure 2). The amplitude of LSPR peak also increases with an increase in the thickness of the film. It was noted during the experiment that the film of thickness ~ 10 nm deposited slowly provides a lower bandwidth LSPR peak at ~ 790 nm in comparison to a broad peak at ~ 981 nm in the case of fast deposition keeping the other parameters constant. This indicates that the position and the profile of the LSPR absorption peaks are not only dependent on the film thickness but also on the deposition rate of the film. Similar behavior has been observed by different groups in the case of gold as well as for the other plasmonic material such as Ag [24-27]. This indicates that each nanostructured film of the gold provides LSPR absorption peak with a finite amplitude and bandwidth depending on the film thickness (Figure 1). The amplitude of LSPR peaks increases with an increase in the number density of AuNPs, whereas the location and the broadening in the peaks are due to the shapes and sizes of the NPs. Normally the LSPR absorption peaks occur as a result of collective oscillation of free electrons in the NPs of thin films, whereas the broadening occurs due to the damping of these collective oscillations. Such observations are explained by the total extinction coefficient of small NPs that are given by the Mie's theory [4-5, 28] as the summation over all the electric and magnetic multipole oscillations contributing to the absorption and scattering of the interacting electromagnetic field. In the
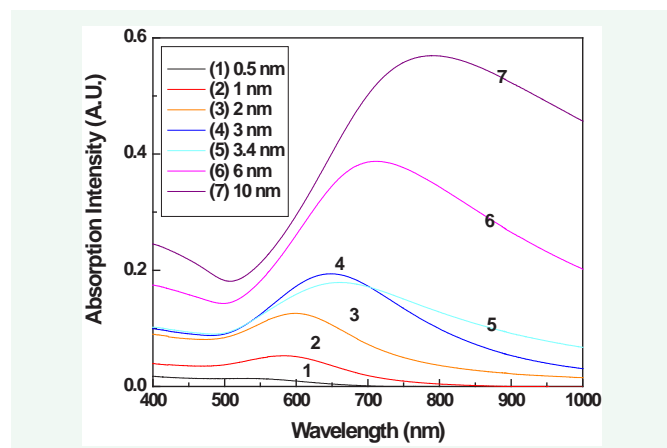
Figure 1 Absorption spectra of the gold thin films of various thicknesses, (1) 0.5, (2) 1, (3) 2, (4) 3, (5) 3.4, (6) 6 and (7) 10 nm.
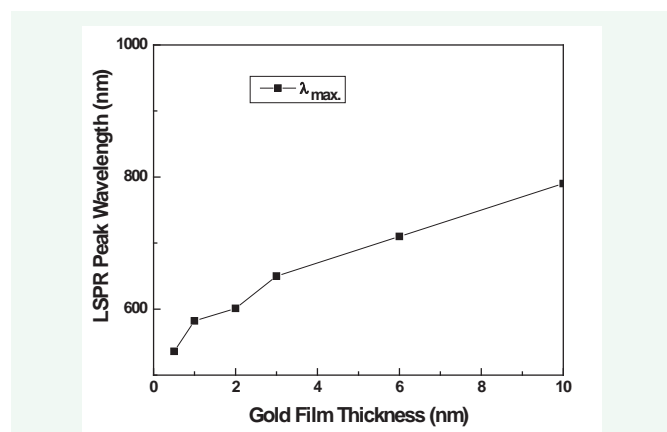

Figure 2 Variation in the localized surface plasmon resonance (LSPR) peak wavelengths with film thicknesses.

case of NPs much smaller than the wavelength of absorbing light only the dipole approximation is considered to be contributing towards the LSPR [5]. However, in the case of larger particles multipole oscillations also play an important role. In the light of Mie's theory the optical absorption spectrum of metallic NPs has been successfully explained after introducing a dielectric function of the material. Considering the free conduction electron in the NPs, the Drude approximation provides an expression for the frequency dependent dielectric function for the material as [26-27].

$$\varepsilon_M = 1 - \frac{\omega_p^2}{\left(\omega^2 + i\gamma\omega\right)} \qquad (1)$$

Where $\omega_p^2 = [ne^2/\varepsilon_0 m_{eff}]$ is the bulk Plasmon frequency, which is dependent on the free electron density n, the charge on electron e, the vacuum permittivity ε_0 and the electron effective mass m_{eff}. Here γ represents the damping constant, which equals the plasmon bandwidth for the case of a perfect free electron gas in the limit of $\gamma \ll \omega$.

The spectroscopic characterization of such films provides information about the collective response of the NPs, which has a

certain distribution of sizes and the shapes of the NPs in the thin films. In this case the absorption maximum of the LSPR depends mainly on the number density of the NPs present in the film. Normally, all the thin films have large number of NPs of different sizes and shapes depending on the thickness of thin films. These small and the large size NPs present in the films act as dipoles and multipoles respectively under the effect of electromagnetic radiation. In the case of large size of NPs the LSPR peak position shifts to longer wavelength side as a result of dominant multipole oscillation. This seems to be the reason behind the shift in LSPR peak towards higher wavelength side with an increase in the film thickness (Figure 1). Similar shift in the LSPR peaks has been reported by many researchers experimentally as well as theoretically [29-31]. However, an interesting behavior of NPs in thin films has been reported by Kundu [32]. He found that the AuNPs in the Langmuir-Blodgett film reorganize its position with time, so that the films become more compact with a decrease in its thickness. Even the coupling between the AuNPs increases due to decrease in the inter-particle distance after its reorganization, which results a red shift in the plasmon peak wavelength. In the present experiment also inter-particle distance decreases with an increase in the film thickness either due to an increase in the number density or due to an increase in the size of the NPs. This is also contributing towards shift in LSPR to higher wavelength side. This indicates that not only the shapes but the sizes of the NPs also play an important role in deciding the location of the LSPR peak, which is in agreement with the reported results [29]. In case the AuNPs are having the shape of nanorods, the LSPR absorption shows two peaks corresponding to the oscillation of the free electrons along (longitudinal mode) and perpendicular (transverse mode) to the long axis of the nanorods. Normally, the AuNPs show transverse mode resonance peak at ∼520 nm, which is coincident with the LSPR peak observed due to the spherical AuNPs. In this case the resonance peak due to the longitudinal mode is observed red shifted and is found strongly dependent on the aspect ratio (AR) R (Length of the rod divided by the diameter of the rod) of the nanorod [33].

After above discussion about the relation between the parameters of AuNPs with amplitude and the location of LSPR peaks. It is important to discuss about the broadening in the LSPR peaks and its dependence on the parameters of AuNPs. The bandwidth of the LSPR peak is defined by the damping parameter γ as given in eq. 1. Normally γ is found dependent on the NPs radius r [34, 35] and can be written as

$$\gamma(r) = \gamma_0 + \frac{Av_F}{r} \qquad (2)$$

Where γ_0 is the bulk damping constant, v_F is the velocity of the electrons at the Fermi energy, and A is a theory dependent parameter that includes details of scattering process. Lot of theoretical work has been performed earlier to define these relations [30]. It has been found that the LSPR bandwidth shows two types of behavior [4-5, 30]. In the case of intrinsic size region (small nanoparticles < 25 nm of radius) the resonance damping shows 1/r dependence and the bandwidth decreases with an increase in the particle size (r). In other case the bandwidth of the collection of NPs increases with an increase in the size (r) of the collection of NPs. This leads to an inhomogeneous polarization

of the NPs by the electromagnetic field, where the broadening of the plasmon band is found due to retardation effect [5]. Even the excitation of multipole modes that peaks at different energies also contributes to the broadening in the LSPR peak. The present experiment shows that the bandwidth of LSPR increases with an increase in the film thickness from 0.5 to 10 nm (Figure 1), which falls under the second category. It is well known that an increase in the film thickness increases the density as well as sizes of the NPs along with certain changes in its shapes, which increases the particle-particle interaction in the films due to decrease in the inter-particle separation. This will also contribute to the broadening in the LSPR peaks. All these factors contribute towards an increase in the bandwidth of the LSPR of thin films. This indicates that an increase in the bandwidth of LSPR peak with the film thickness in the present experiment seems to be occurring as a result of change (increase) in the shapes, sizes and the number density of the NPs [29]. Serrano et al. [24] and Cesario et al., [31] have also demonstrated that in the case of comparatively thick film (high particle density), interaction between the localized and the extended surface plasmons also induce similar changes in the optical absorption spectra (increase in the bandwidth) of the AuNPs due to close proximity of nanoislands with each other.

The above discussions indicate that the shapes and the sizes of the NPs as well as its density in each film play an important role during the collective oscillations of free conduction electrons in providing the specific LSPR peaks in the absorption spectra of the thin films. However, any change in the local environment particularly the refractive index of the surrounding medium also affects the position of LSPR peak, which makes these films a good plasmonic sensor for organic and biological samples. It has been reported that a film having narrow bandwidth in its LSPR peak provides higher sensitivity and large near field enhancement useful for the sensors and the surface enhanced spectroscopy. Normally, the nanorods with high AR value show the narrowest bandwidth in comparison to the nanosphere [20]. It shows that optimization of thin films parameters that decides the size, shape and the number density of NPs in films will increase the sensitivity of such sensors [20, 29]. Finally, this indicates that the study of surface morphology of the films and its correlation with LSPR can provide better understanding in order to optimize its sensitivity as plasmonic sensor.

Morphological Characterization of gold thin films

It has been discussed above that the LSPR peak not only depends on the film thickness but also on the other film deposition parameters, which decides the morphological features of the film such as the shapes and the sizes of the NPs in the film. This indicates that the AuNPs present in the gold thin films obtained by vacuum evaporation method may also be having different shapes and sizes. Here Figures (3-5) show the TEM images of the gold films as well as distribution of ellipticity (the ratio of major to minor axis) of the NPs for 1, 3 and 6 nm thick films respectively. It shows that the 1 nm thick film has mostly spherical NPs with ellipticity one. As the film thickness increases to 3 nm, the shapes of nanoparticles start changing (ellipticity > 1) but still more number of particles are in spherical shape with ellipticity one (Figure 4). The 6 nm thick film (Figure 5) contains NPs of various other shapes with maximum number of particles

having ellipticity 1.4. The radius distribution shows that the 1 nm thin films has maximum numbers of particles having radius ranging from ~1.75 to 2.75 nm, whereas it is ~4-5 and ~5-7 nm for 3 and 6 nm thick films respectively. This indicates that the film with less thickness (< 6 nm) has NPs of nearly spherical shape, which got distorted as the film thickness increases. Here Figure (3-5) shows that each film has different distribution of ellipticity of the NPs, which changes with an increase in the film thickness. In fact, the average ellipticity increases with an increase in the film thickness. Particularly, Figure (5b) shows the distribution of ellipticity for the film of thickness ~6 nm, which has average ellipticity of ~1.7. Figure (6) shows 2 and 3 D AFM pictures of the ~3 nm thick film. No clear base structure is seen in two dimensional AFM pictures of the films. However 3D picture shows an increase in the height of the nanoparticles. Figure (7) shows 2 and 3 dimensional AFM pictures of the ~6 nm gold film. Here 2 D picture clearly shows the presence of some triangular shaped NPs, whereas 3 D picture shows clear vertical structure of the NPs in the form of nanorods. This indicates that the sufficient numbers of nanorods are present in ~6 nm thick film. The coverage of the surface area by the NPs increases with an increase in the film thickness (Figure 3-5), which is measured in the term of volume fraction. The measured roughness parameters for the ~3 and ~6 nm films using AFM are shown in Table (1). This shows that the average heights as well as the average and rms roughness of the films increase with an increase in the film thickness from ~3 to ~6 nm. The above results show that the LSPR peak wavelength shifts to longer wavelength with an increase in the size of nanoparticles and the surface roughness of the thin films. Similar observations have been reported earlier, where different island size and roughness in the films were created by annealing the thick films [21]. These results confirm that all the parameters of the thin film preparation such as deposition rate, deposition process, annealing temperature of the films and its atmosphere play an important role in deciding the surface roughness and /or the size of NPs present in the thin film and consequently its LSPR wavelength [23-25].

It has been observed in the last section that the LSPR peak wavelength red shifts with an increase in the film thickness. Therefore, a correlation between the LSPR peak wavelength of the films and its surface morphology can provide important information. Figure (8) shows variation in the LSPR peak wavelength of the films with an increase in the average ellipticity, volume fraction and the aspect ratio (AR) of the NPs in the films. The nanorods present in the films are in the form of non-cylindrical shape with an elliptical (triangular) base [18]. Therefore, AR of the NPs has been defined here as the ratio of the film thickness and the average ellipticity of the nanoparticles in that film. A comparison shows that the LSPR peak wavelengths have best linear fit with the AR of the NPs in the thin films, whereas ellipticity and the volume fraction deviates from linearity near ~10 nm film thickness. This indicates that the redshift in the LSPR peak wavelength is mainly dependent on the surface coverage by the NPs as well as on the AR of the NPs in films. However, the best linear fit with the AR indicates that the height of NPs also play an important role in deciding the LSPR peak along with its size in X-Y plane as reported earlier [25]. The AFM images of the ~6 nm film show that the sufficient numbers of NPs are present
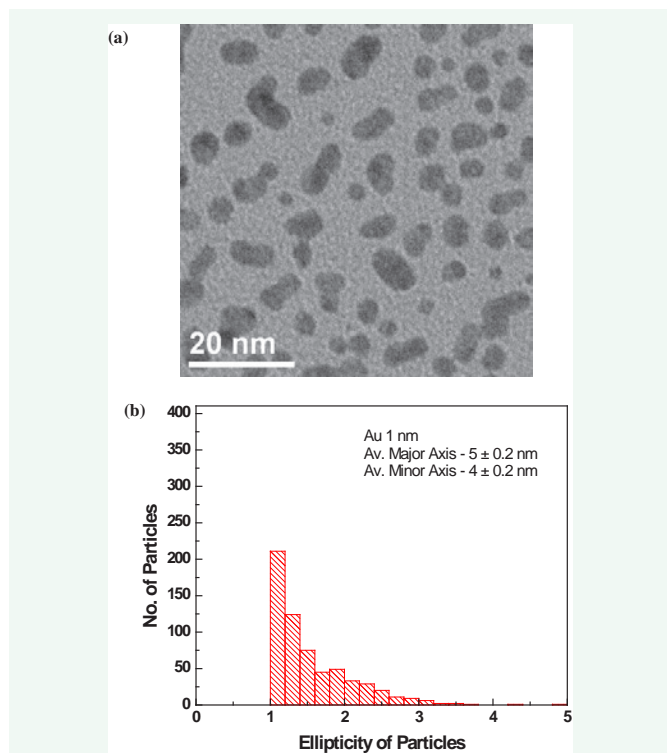
SciMedCentral

Figure 3 Variation in the size and the shape of nanoparticles in the gold film of 1 nm thickness, (a) TEM micrograph, (b) Histogram of variation in the ellipticity of the nanoparticles on substrate.
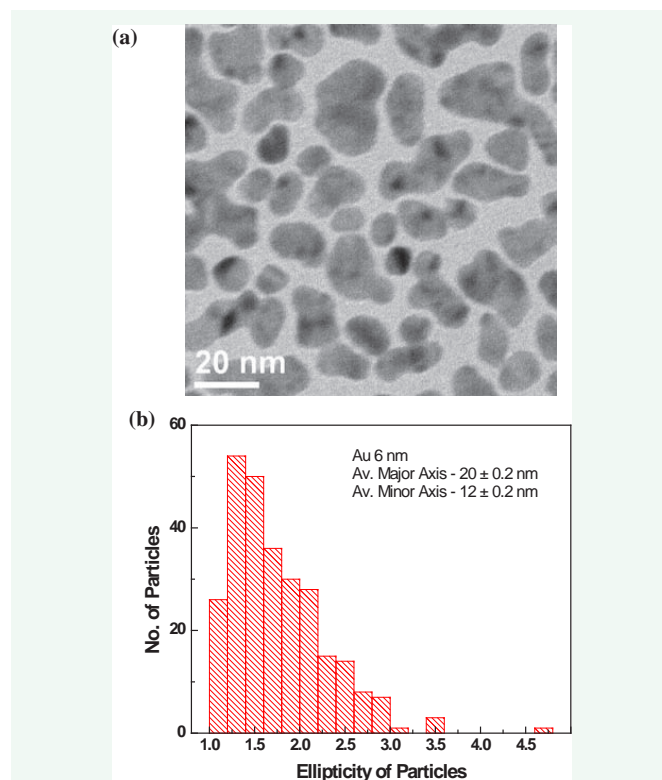

Figure 4 Variation in the size and the shape of nanoparticles in the gold film of 3 nm thickness, (a) TEM micrograph, (b) Histogram of variation in the ellipticity of the nanoparticles on substrate.
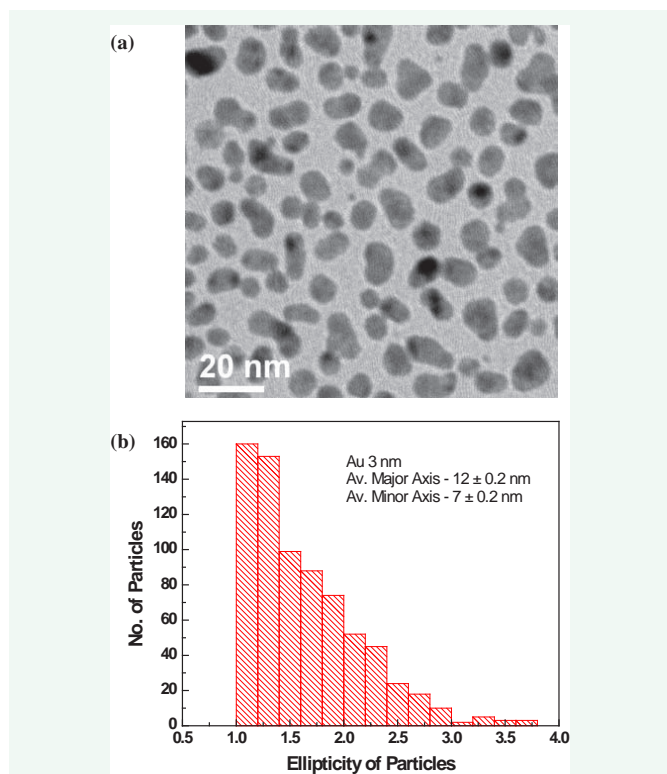

Figure 5 Variation in the size and the shape of nanoparticles in the gold film of 6 nm thickness, (a) TEM micrograph, (b) Histogram of variation in the ellipticity of the nanoparticles on substrate.

Table 1: Data of surface roughness measurement of gold thin film using AFM.

Gold Film Thickness (t)	Pk-Pk Roughness (nm)	Average Roughness (nm)	RMS Roughness (nm)
3 nm (1x1 µm)	3.05	0.26 ± 0.02	0.34 ± 0.02
6 nm (1x1 µm)	6.10	0.51 ± 0.02	0.69 ± 0.02

in the form of nanorods. In fact the formation of nanorods becomes dominant for the film thickness of > 3 nm. This is in agreement with the earlier reported results that the formation of nanorod structure during vapor deposition process is possible after crossing the percolation transition [25, 36]. The growth of the nanorods seems to be possible due to the slow deposition rate, where evaporated material got stacked one over the other without any diffusion. This indicates that the NPs present on the film of different thicknesses may be having nanorods of different aspect ratio with a certain possible distribution.

Refractive Index of the surrounding medium

The optical property of thin film is mostly decided by its dielectric permittivity ε (as discussed in section 3.1) which consists of two important parameters as coefficient of refraction (n) and the extinction coefficient (k). In the case of thin films having NPs, the effective dielectric permittivity can be defined in terms of volume fraction and the polarizability of the metallic NPs [37-38]. The polarizability of any film is proportional to the number of NPs times volume of each NP present on the film, that
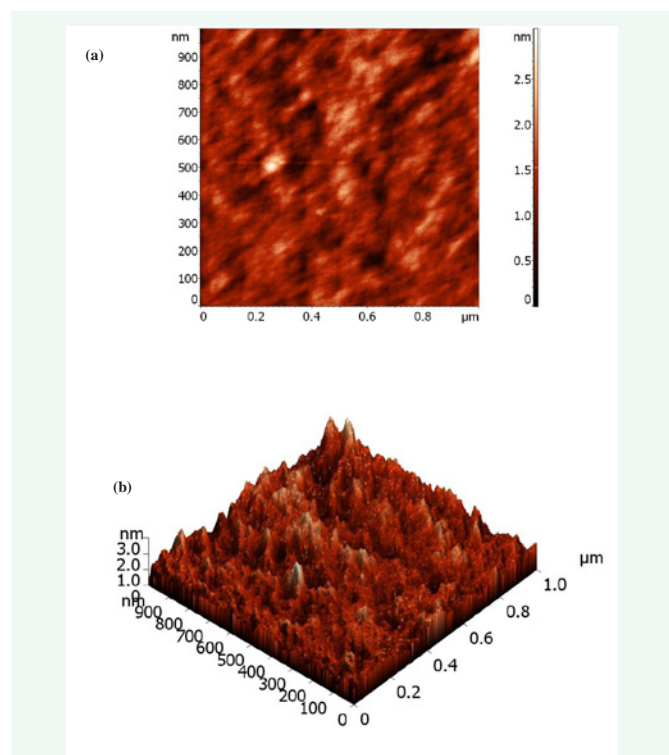
SciMedCentral

Figure 6 AFM micrograph of the surface structures in 3 nm thick gold film, (a) 2 D picture, (b) 3 D picture.
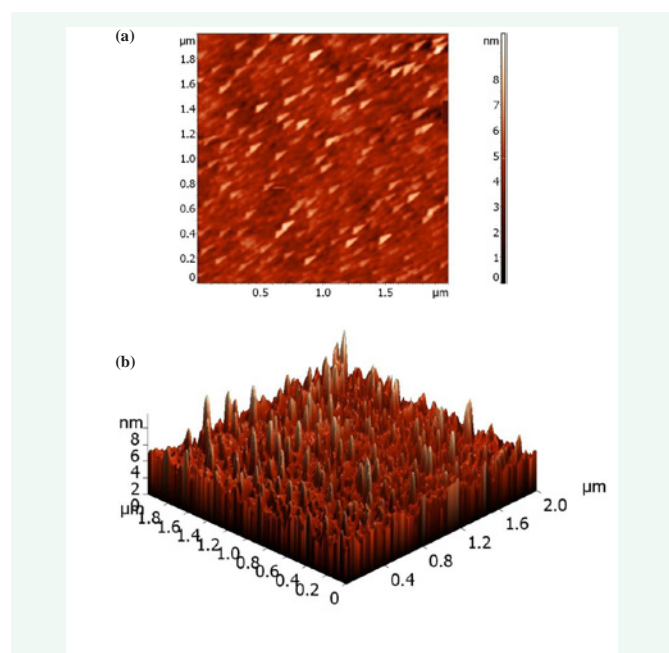

Figure 7 AFM micrograph of the surface structures in 6 nm thick gold film, (a) 2 D picture, (b) 3D picture.

is, fractional volume (F) of the film. Normally, this is considered as the coverage area of the film by NPs It has been proved to be more important parameter in expressing the optical properties of the films having different sizes of the NPs. Based on the free electron model of the metal, it has been reported that the

LSPR peak wavelength λ_m and the wavelength of the plasmon resonance peak of the bulk metal λ_p (for gold 131 nm) is related with the volume fraction (F) as well as the refractive index n_s of the effective medium surrounding the films. This relation can be written as [38].

$$\lambda_m = \lambda_p \left[1 + \left(\frac{2+F}{1-F} \right) n_s^2 \right]^{\frac{1}{2}} \tag{3}$$

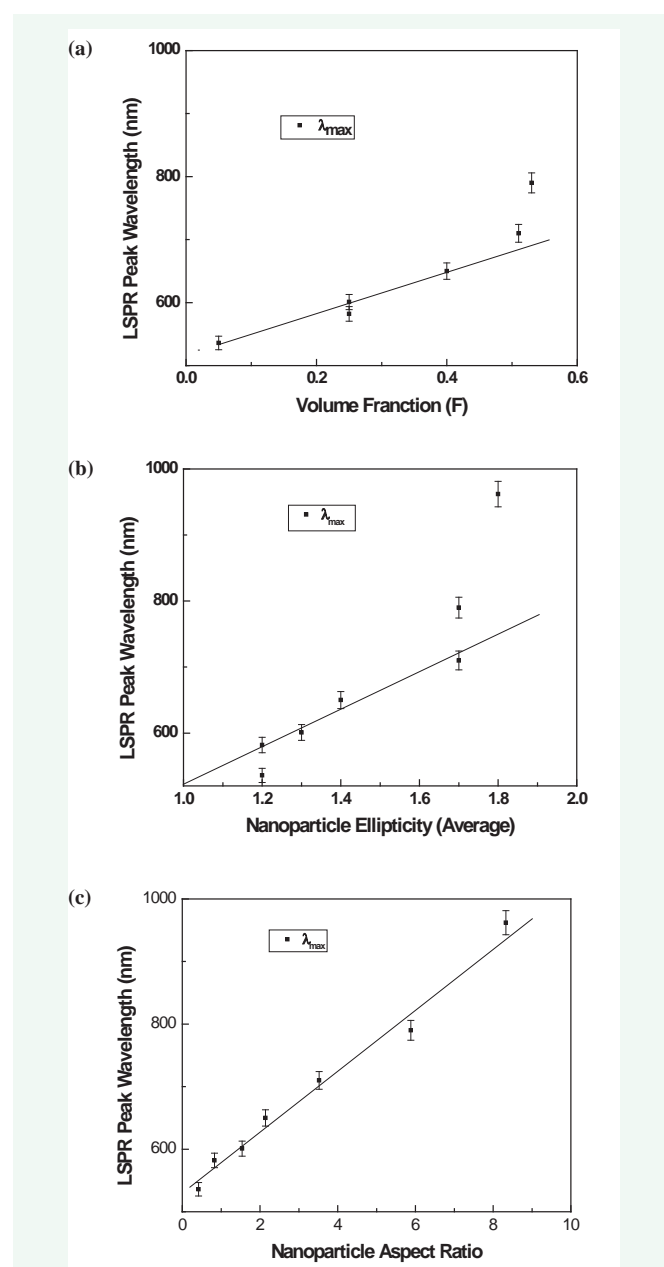This is a simple analytical approximation for the LSPR

Figure 8 Variation in the localized surface plasmon resonance peak wavelength with, (a) Volume fraction of the nanoparticles in the films, (b) Average ellipticity of the nanoparticles in the films, (c) Aspect ratio of the nanoparticles in the films.

peak shift within the frame work of Maxwell Garnet theory [37]. This clearly indicates that not only the fractional volume (number density of NPs in the film) but the refractive index of the surrounding media around the NPs also affects the LSPR wavelength and has been found as an important parameter. For a fixed F of a thin film any change in n_s will provide corresponding change in the LSPR wavelength. This property of the thin film can be used as a sensor for the detection of any organic or biological sample. It has been reported earlier that eq.-3 fits the experimental data very well in the case of indium, silver and the gold nanostructured thin films [18, 35]. In fact the surrounding medium around the gold NPs are air, glass and gold itself in the present experiment. In this case, the coverage of films by NPs (F) and the corresponding LSPR peak wavelength λ_m change with change in the thickness of films, which is affecting the value of n_s. Based on this idea the values of n_s have been obtained for each thickness of the gold thin films using eq.-3 in order to find its correlation with the parameters of the film such as volume fraction, ellipticity and aspect ratio of the NPs. Figure 9a indicates that values of n_s decreases with an increase in the film thickness except for the value of higher film thickness (~10nm). This variation is in close agreement with the results reported earlier [22]. However, the deviation in the data for ≥ 10 nm thick film may be because this film becomes semi-continuous and subsequently loses its NP character. The variation in refractive index of the surrounding medium n_s with the AR values of the NPs in the film is shown in Figure (9b). Similar variations in the values of n_s are noted with the change in ellipticity and the volume fraction. Figure (10) shows that the values of n_s decrease linearly with an increase in the LSPR peak wavelength. Another observation is that the value of n_s decreases with an increase in the roughness of the film surface (Table 1), that is, with an increase in the size / AR of the nanorods. Here one can say that the values of refractive index of surrounding medium (n_s) for a particular film will change once we fill the inter-particle spacing (over coating the thin film) with a material of different refractive index (organic or biological samples), which is air in the present case [39]. In such a situation the optical properties of the composite film as well as the value of n_s can provide information about the materials over coated on the film. This indicates that such films can act as a sensor for the over coated materials. The refractive index sensitivities of these films have been studied for the over coating of Rh6G and is found that the LSPR peaks show a change of ~300 nm per unit change in the refractive index [40]. However, it is important to increase the change in the values of λ_m per unit change in the refractive index of the surrounding medium that is the refractive index sensitivity of sensor for the samples. This may be possible by changing the surface morphology of the films either by changing its preparation technique or by changing the material of the film. Recently, a silver nanoparticle plasmonic grating has been developed as a substrate for surface enhanced Raman spectroscopy (SERS), which provided an enhancement in Raman signal from Rh6G dye sample by two orders of magnitude [41]. However, further increasing the sensitivity of such plasmonic sensors is a matter of further investigation.

CONCLUSIONS

The nanostructured gold thin films show LSPR in its absorption spectra at the wavelengths ranging from visible to
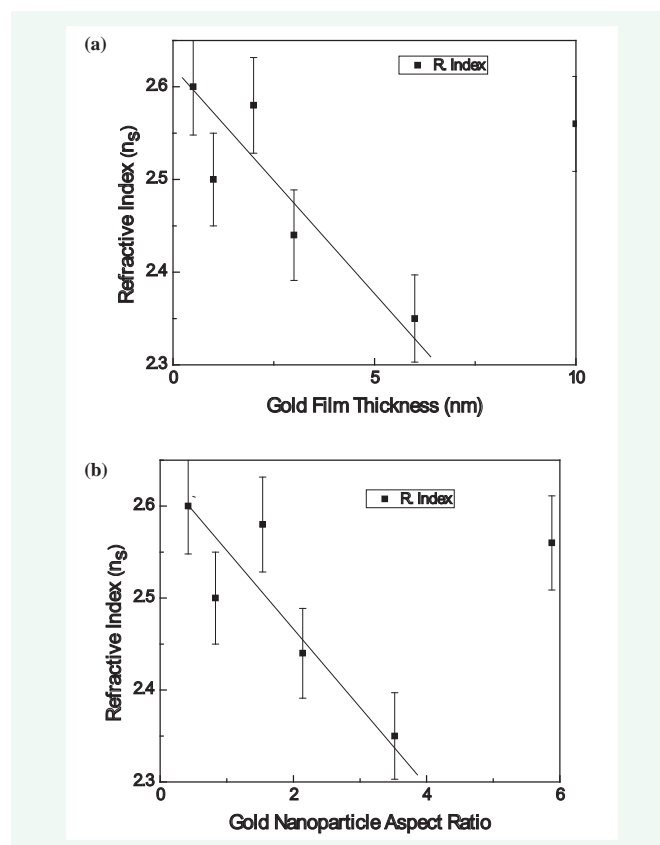
Figure 9 Variation in the refractive index of the thin films with, (a) Film thickness, (b) Aspect ratio of the nanoparticles in the thin films.
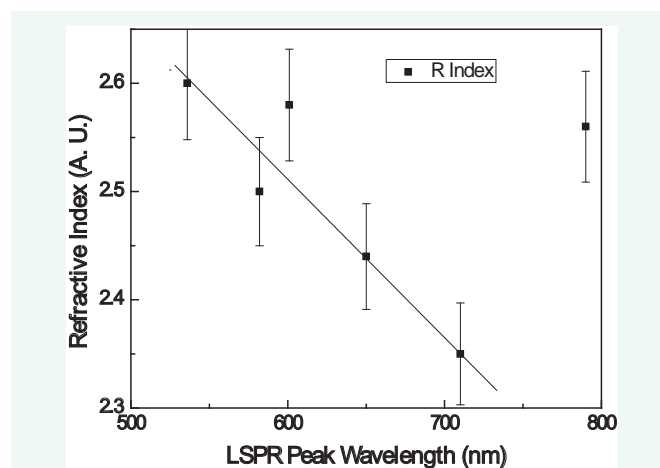
Figure 10 Variation in the refractive index of the thin films with LSPR peak wavelength.

near infrared wavelength depending on the thickness of films. Each parameter of the film such as the volume fraction, the sizes and the shapes of the NPs as well as the surface roughness have an important role in deciding the optical properties of the thin films. A good correlation has been found between the optical properties of the thin films such as LSPR and the refractive index of the surrounding medium with the surface morphology of films. The above results further indicate that the Mie [4-5] and the

SciMedCentral

Maxwell Garnet theory [31] explains the observations mainly for the gold thin films having NPs of nearly spherical shape having ellipticity close to one. Such thin films can be useful as a substrate either for the study of surface enhanced spectroscopy or as a good refractive index sensor for organic or biological samples. However, further investigation is required in this direction to obtain a plasmonic film with better surface morphology and optical properties in order to have a sensor with better sensitivity for various applications.

REFERENCES

1. Maier SA. Plasmonics: Fundamentals and Applications, New York. Springer Science; 2007.

2. Hutter E, Fendler JH. Exploitation of localized surface plasmon resonance. Adv Mater. 2004; 16; 1685-1706.

3. Haes AJ, Haynes CS, Mc Farland AD, Schatz GC, Van Duyne RP, Zon S. Plasmonic materiasl for surface enhanced sensing and spectroscopy. MRS Bulletin. 2005; 30: 368-375.

4. Bohren CF, Huffman DR. Absorption and scattering of light by small particles. New York: Wiley-InterScience; 1983.

5. Kreibig U, Vollmer M. Optical properties of metal clusters. Springer Series in Material Science. Berlin: Springer Verlog. 1995.

6. Cai W, Shalaev V. Optical metamaterials: Fundamentals and applications. New York: Sringer Science. 2010.

7. Gu Y, Li Q, Xiao J, Wu K, Wang GP. Plasmonic metamaterials for ultra-sensitive refractive index sensing at near infrared. J Appl Phys. 2011; 109; 023104.

8. Kelly KL, Coronado E, Zhao LL, Schatz GC. The optical properties of metal nanoparticles: the influence of size, shape and dielectric environment. J Phys Chem. 2003; 107: 668-677.

9. El-Sayed MA. Some interesting properties of metals confined in time and nanometer space of different shapes. Acc Chem Res. 2001; 34: 257-264.

10. Haynes CL, Van Duyne RP. Nanosphere lithography: A versatile nanofabrication tool for studies of size dependent nanoparticle optics. J Phys Chem. 2001; 105: 5599-5611.

11. Jain PK, Huang X, El-Sayed IH, El-Sayed MA. Noble metals on the nanoscale: optical and photothermal properties and some applications in imaging, sensing, biology, and medicine. Acc Chem Res. 2008; 41: 1578-1586.

12. Dykman LA, Khlebtsov NG. Gold nanoparticles in biology and medicine: recent advances and prospects. Acta Naturae. 2011; 3: 34-55.

13. Chen Y, Preece JA, Palmer RE. Processing and characterization of gold nanoparticles for use in plasmon probe spectroscopy and microscopy of biosystems. Ann N Y Acad Sci. 2008; 1130: 201-6.

14. Hoa XD, Kirk AG, Tabrizian M. Towards integrated and sensitive surface plasmon resonance biosensors: a review of recent progress. Biosens Bioelectron. 2007; 23: 151-60.

15. Moskovits M. Surface enhanced spectroscopy. Rev Mod Phys. 1985: 57: 783.

16. Gray SK. Surface plasmon enhanced spectroscopy and photochemistry. Plasmonics. 2007; 2: 143-146.

17. Nie S, Emory SR. Probing Single Molecules and Single Nanoparticles by Surface-Enhanced Raman Scattering Science. 1997; 275: 1102-1106.

18. Rai VN, Srivastava AK, Mukherjee C, Deb SK. Surface enhanced absorption and transmission from dye coated gold nanoparticles in thin films. Appl Opt. 2012; 51: 2606-2615.

19. Lee TH, Lee SW, Jung JA, Ahn J, Kim MG, Shin YB. Signal amplification by enzymatic reaction in an immunosensor based on localized surface plasmon resonance (LSPR). Sensors (Basel). 2010; 10: 2045-2053.

20. Huang X, Neretina S, El-Sayed MA. Gold nanorods: from synthesis and properties to biological and biomedical applications. Adv Mater. 2009; 21: 4880-4910.

21. Chen M, Horn RG. Refractive index of sparse layers of adsorbed gold nanoparticles. J Colloid Interface Sci. 2007; 315: 814-817.

22. Wang X, Chen KP, Zhao M, Nolte DD. Refractive index and dielectric constant transition of ultra-thin gold from cluster to films. Opt Express. 2010; 18: 24859-24867.

23. Bendevid A, Martin PJ, Wieczorek L. Morphology and optical properties of gold thin films prepared by filtered arc deposition. Thin Solid Films. 1999; 354: 169-175.

24. Serrano A, Rodriguez de la Fuente O, Garcia MA. Extended and localized surface plasmons in annealed Au films on glass substrate. J Appl Phys. 2010; 108: 074303.

25. Gupta R, Dyer MJ, Weimer WA. Preparation and characterization of surface plasmon resonance tunable gold and silver films. J Appl Phys. 2002; 92: 5264.

26. Craighead HG, Glass AM. Optical absorption of small metal particles with adsorbed dye coats. Opt Lett. 1981; 6: 248-50.

27. Rai VN. Optical properties of silver-island films having an overlayer of RhB dye. Appl Opt. 1987; 26: 2395-2400.

28. Kerker M. The scattering of light and other electromagnetic radiation. New York: Academic Press; 1969.

29. Naguez C. Surface plasmons on metal nanoparticles: the influence of shape and physical environment. J Phys Chem. 2007; 111: 3806-3819.

30. Link S, El-Sayed MA. Spectral properties and relaxation dynamics of surface plasmon electronic oscillations in gold and silver nanodots and nanorods. J Phys Chem. 1999; 103: 8410-8426.

31. Cesario J, Gonzalez MU, Cheylan S, Barnes WL, Enoch S, Quidant R. Coupling localized and extended plasmons to improve the light extraction through metal films. Opt Express. 2007; 15: 10533-10539.

32. Kundu S. Inter particle coupling of plasmon fields due to reorganization of Au nanoparticles in Langmuir-Blodgett film. J Appl Phys. 2012; 112: 014323.

33. Link S, El-Sayed MA. Simulation of optical absorption spectra of gold nanorods as a function of their aspect ratio and the effect of the medium dielectric constant. J Phys Chem. 2005; 109: 10531-10532.

34. Kreibig U, Fragstein CV. The limitation of electron mean free pathin small silver particles. Z Phys. 1969; 224: 307.

35. Kreibig U. Kramer Kroning analysis of optical properties of small silver particles. Z phys. 1970; 234: 307.

36. Gadenne P, Rivol JC, Optical properties of nanostructured random media (Ed) Shalaev VM, New York: Springer; 2002.

37. Maxwell Garnett JC. Colours in metal glasses and in metallic films. Philos Trans R Soc. 1904; 385: 203.

38. Treu JI. Mie scattering, Maxwell Garnett theory, and the Giaever immunology slide. Appl Opt. 1976; 15: 2746-2750.

39. Lee KS, El-Sayed MA. Dependence of the enhanced optical scattering efficiency relative to that of absorption for gold metal nanorods on aspect ratio, size, end-cap shape and medium refractive index. J Phys Chem. 2005; 109: 20331-20338.

40. Rai VN, Srivastava AK, Mukherjee C, Deb SK. Localized surface plasmon resonance and refractive index sensitivity of vacuum evaporated nanostructured gold thin films. Ind J Phys. 2016; 90: 107-116.

41. Sudheer, Tiwari P, Bhartia S, Mukherjee C, Singh MN, Sinha AK, et al. Fabrication of large area plasmonic nanoparticle grating structure on silver halide based transmission electron microscope film and its application as a surface enhanced Raman spectroscopy substrate. J

Cite this article